

Fig. 1 High-Level Overview of the proposed taxonomy



Fig. 2(a) System interface of MV2Net [20]: many simple filters such as sliders, drop-down menus and labels are distributed within the various views of the system.

L. Shi et al. Mvnet: Multi-variate multi-view brain network comparison over uncertain data.

<https://doi.org/10.1109/TVCG.2021.3098123>

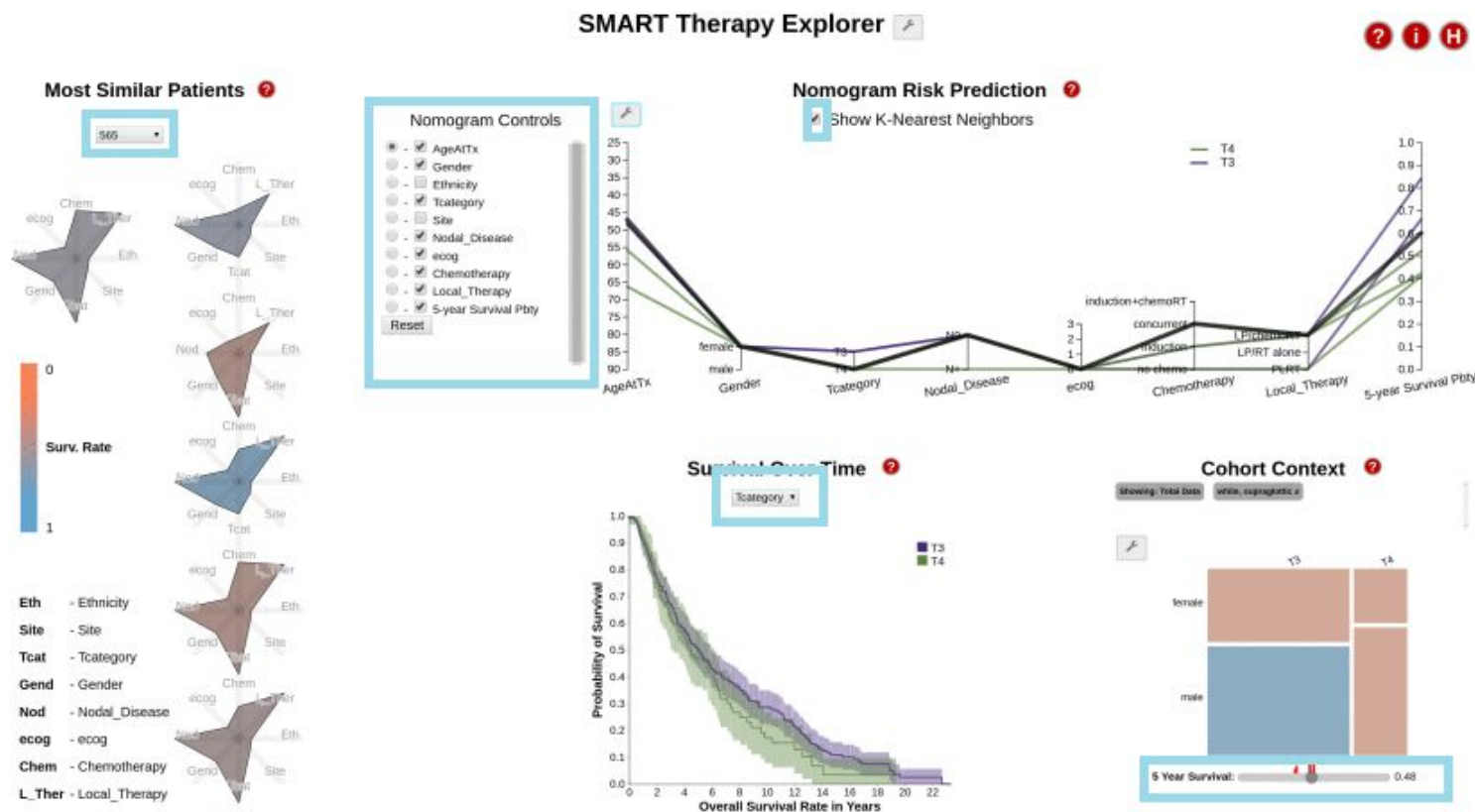


Fig. 2(b) System interface proposed by Marai et al. [21]: many simple filters are distributed within the various views of the system and also in the "Cohort Context" view you can see the scented widget.

G. E. Marai et al. Precision risk analysis of cancer therapy with interactive nomograms and survival plots.

<https://doi.org/10.1109/TVCG.2018.2817557>

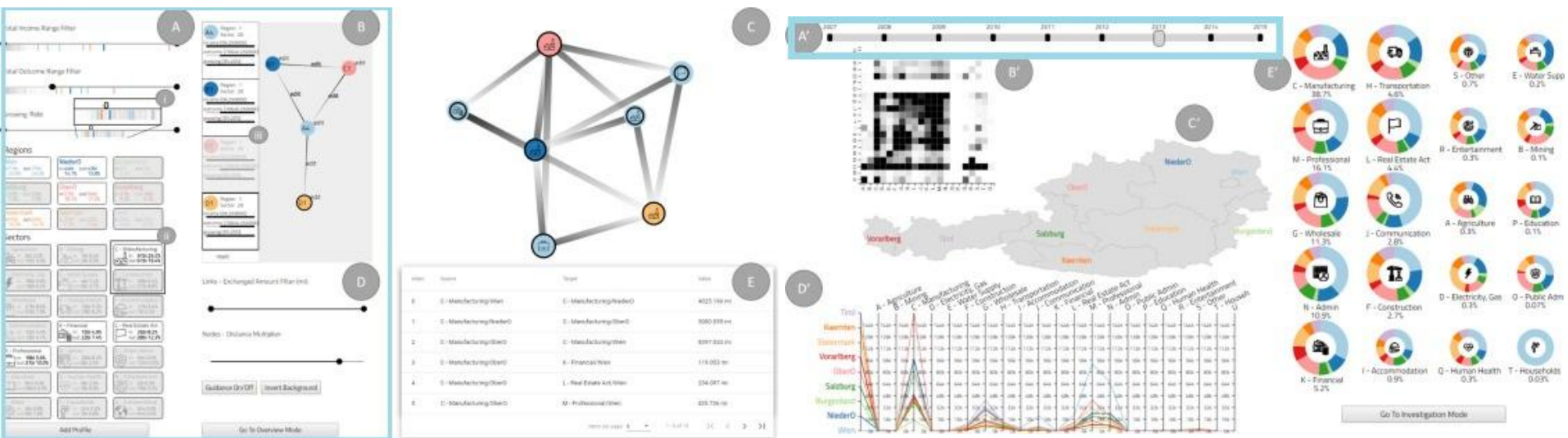


Fig. 2(c-d) Hermes system interfaces [22]: section A and B show the implemented filter with feedback and guidance

R. A. Leite et al. Hermes: Guidance-enriched visual analytics for economic network exploration.

<https://doi.org/10.1016/j.visinf.2020.09.006>

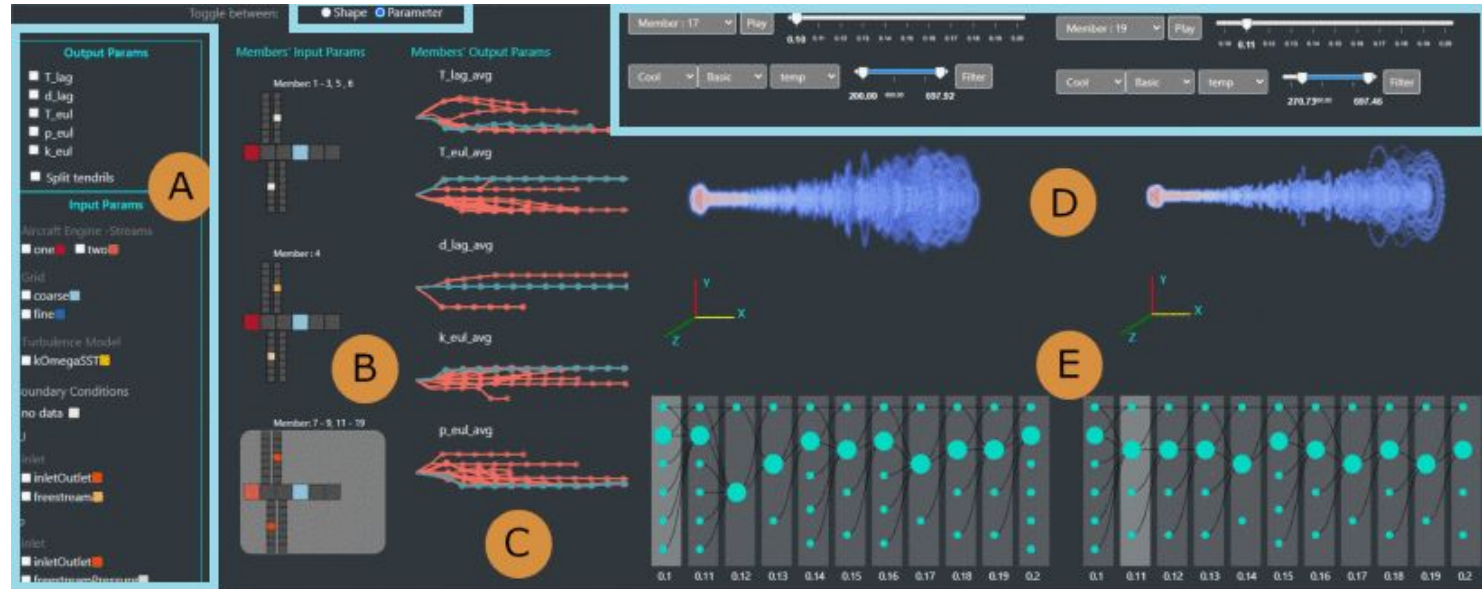


Fig. 2(e) System interface proposed by Nipu et al. [23]: it can be seen that both in section A and in section D there are simple filters

N. Nipu et al. Visual analysis and detection of contrails in aircraft engine simulations.

<https://doi.org/10.1109/TVCG.2022.3209356>



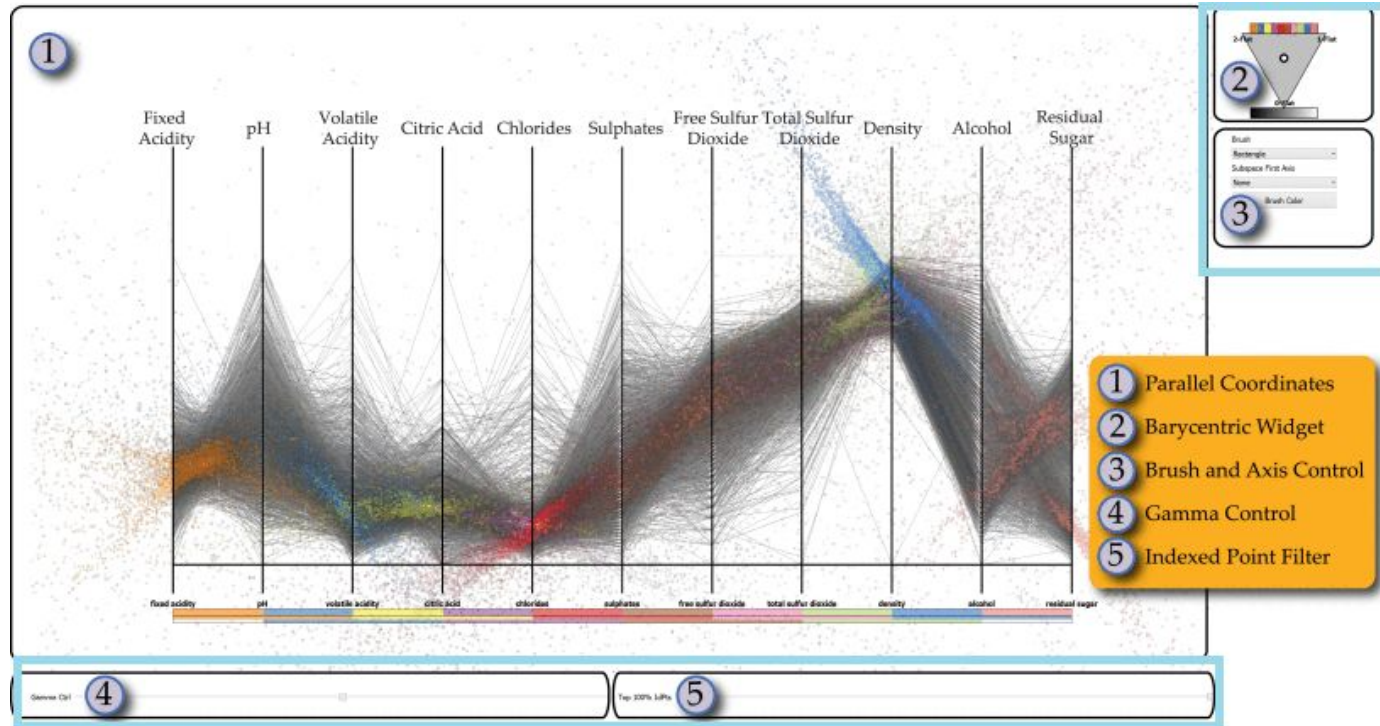


Fig. 2(f) System interface proposed by Zhou and Weiskopf [24]: it can be seen that sections 2-5 are all filters but in particular section 2 presents a complex filter.

L. Zhou and D. Weiskopf. Indexed-points parallel coordinates visualization of multivariate correlations.

<https://doi.org/10.1109/TVCG.2017.2698041>

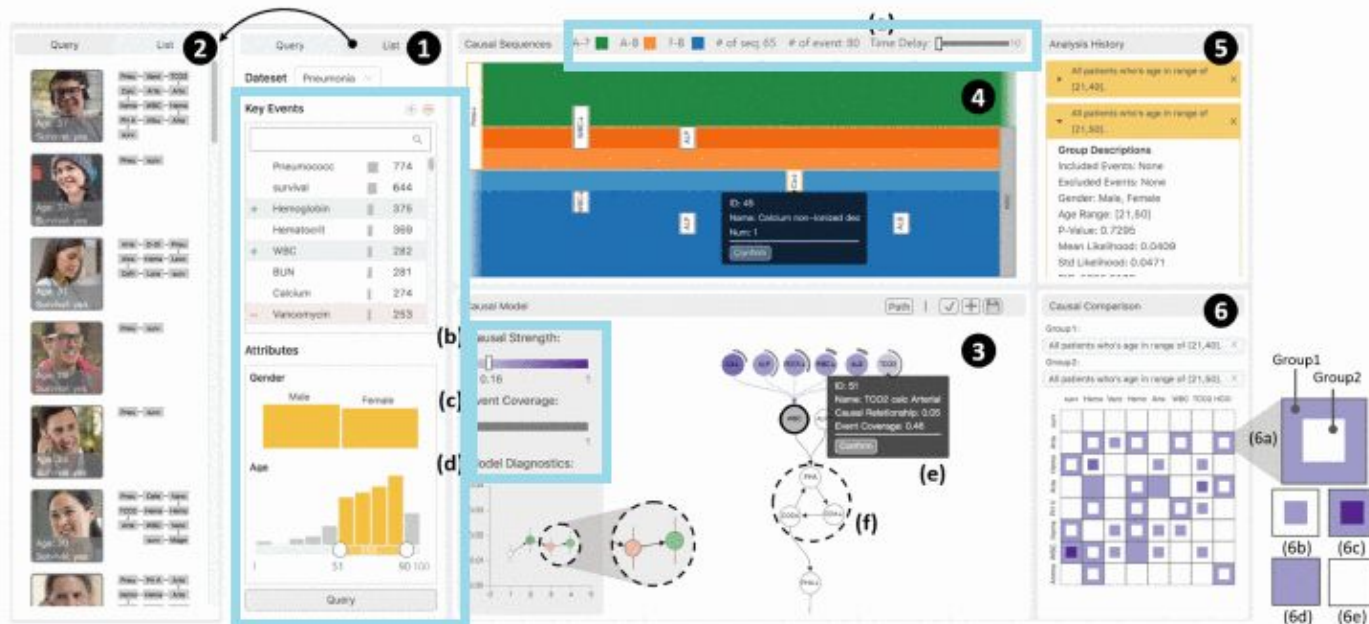


Fig. 3(a) System interface of SeqCausal [41]: in section 1 you can find all the filters with feedback present in the system.

Z. Jin et al. Visual causality analysis of event sequence data.

<https://doi.org/10.1109/TVCG.2020.3030465>

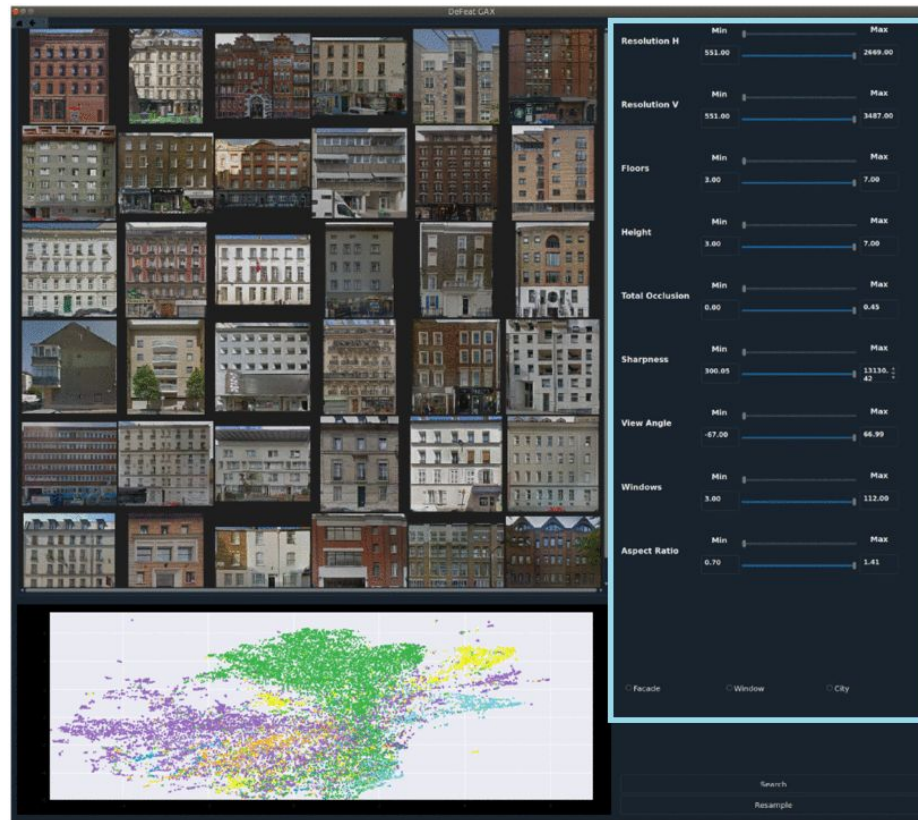


Fig. 3(b) System interface proposed by Zhu et al. [47]: on the right side you can see an area dedicated to filters (all of a simple type)

P. Zhu et al. Large-scale architectural asset extraction from panoramic imagery

<https://doi.org/10.1109/TVCG.2020.3010694>



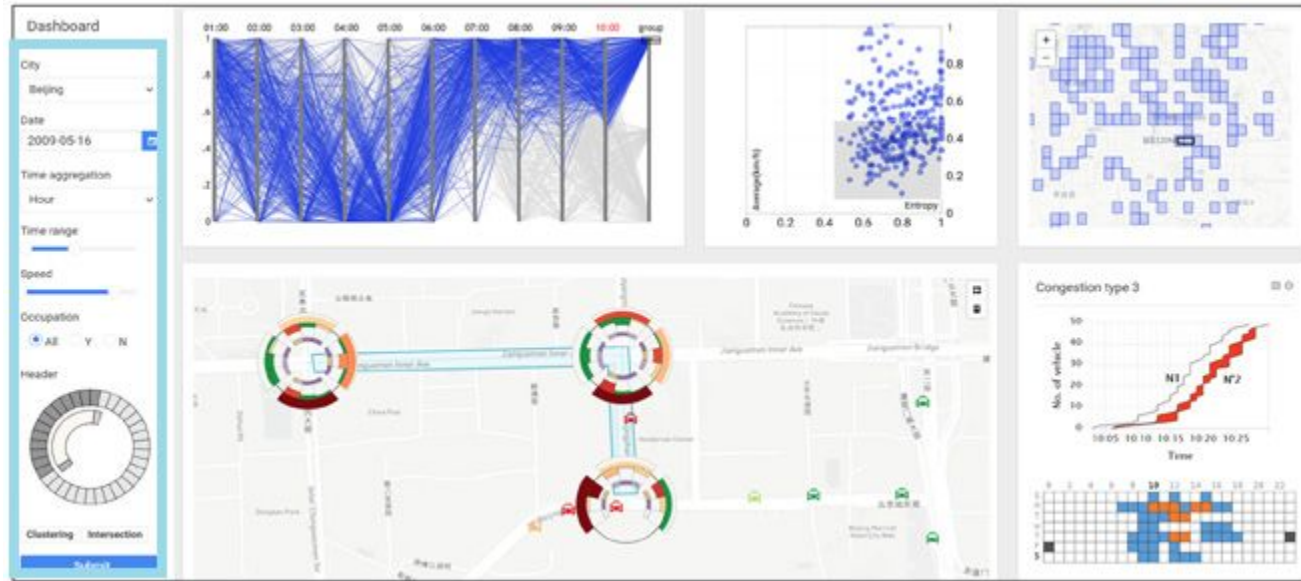


Fig. 3(c) System interface proposed by Pi et al. [49]: in the dashboard you can see the complex filter called header at the bottom

M. Pi et al. Visual cause analytics for traffic congestion.

<https://doi.org/10.1109/TVCG.2019.2940580>

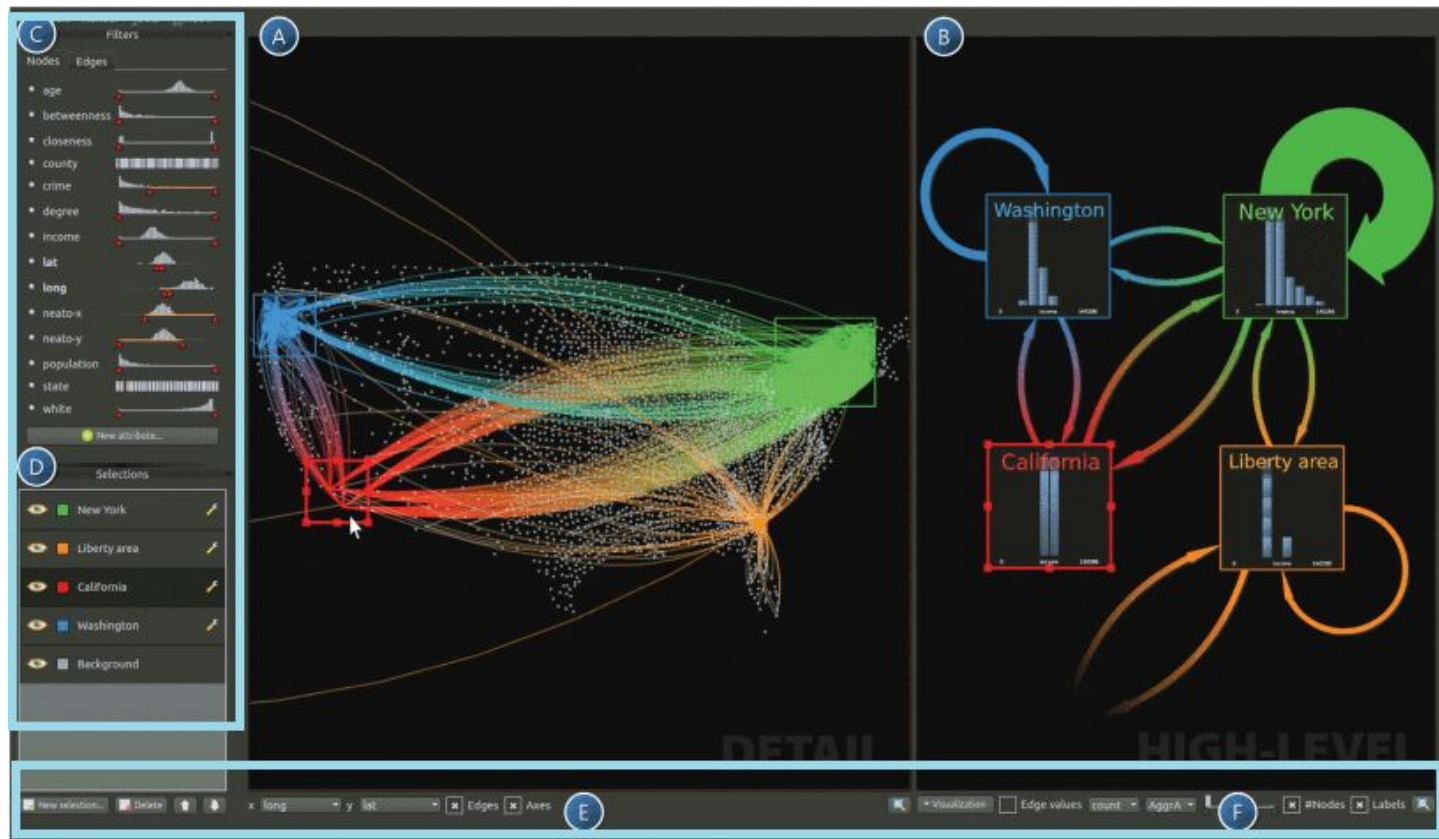


Fig. 3(d) System interface proposed by van den Elzen and van Wijk [50]: in section C you can see the implemented scented widgets

S. van den Elzen and J. J. van Wijk. Multivariate network exploration and presentation: From detail to overview via selections and aggregations.

<https://doi.org/10.1109/TVCG.2014.2346441>

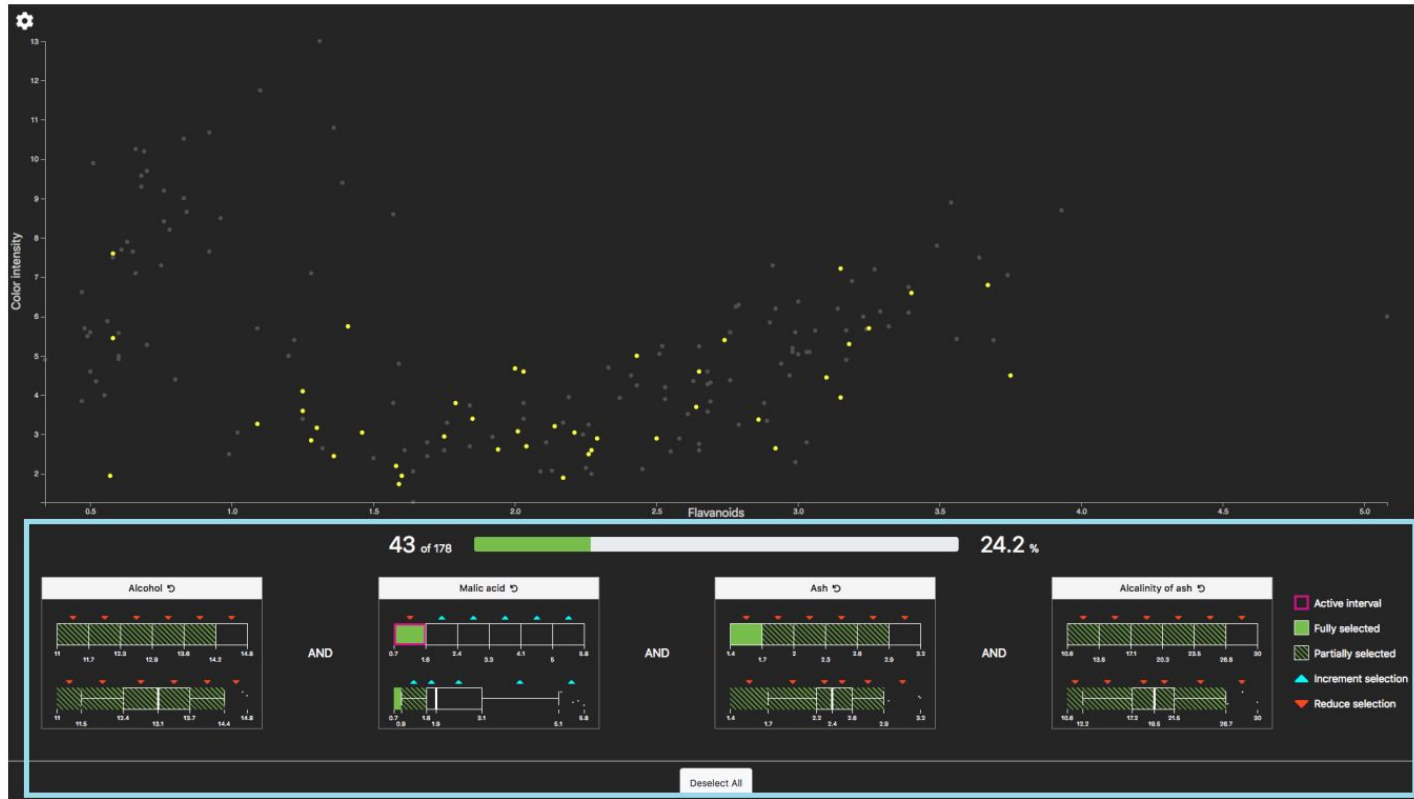


Fig. 3(e) System interface implemented by Angelini et al. [11]: in the lower part you can see the filters with feedback and guidance

M. Angelini et al. Crosswidgets: Enhancing complex data selections through modular multi attribute selectors.

<https://doi.org/10.1145/3399715.3399918>

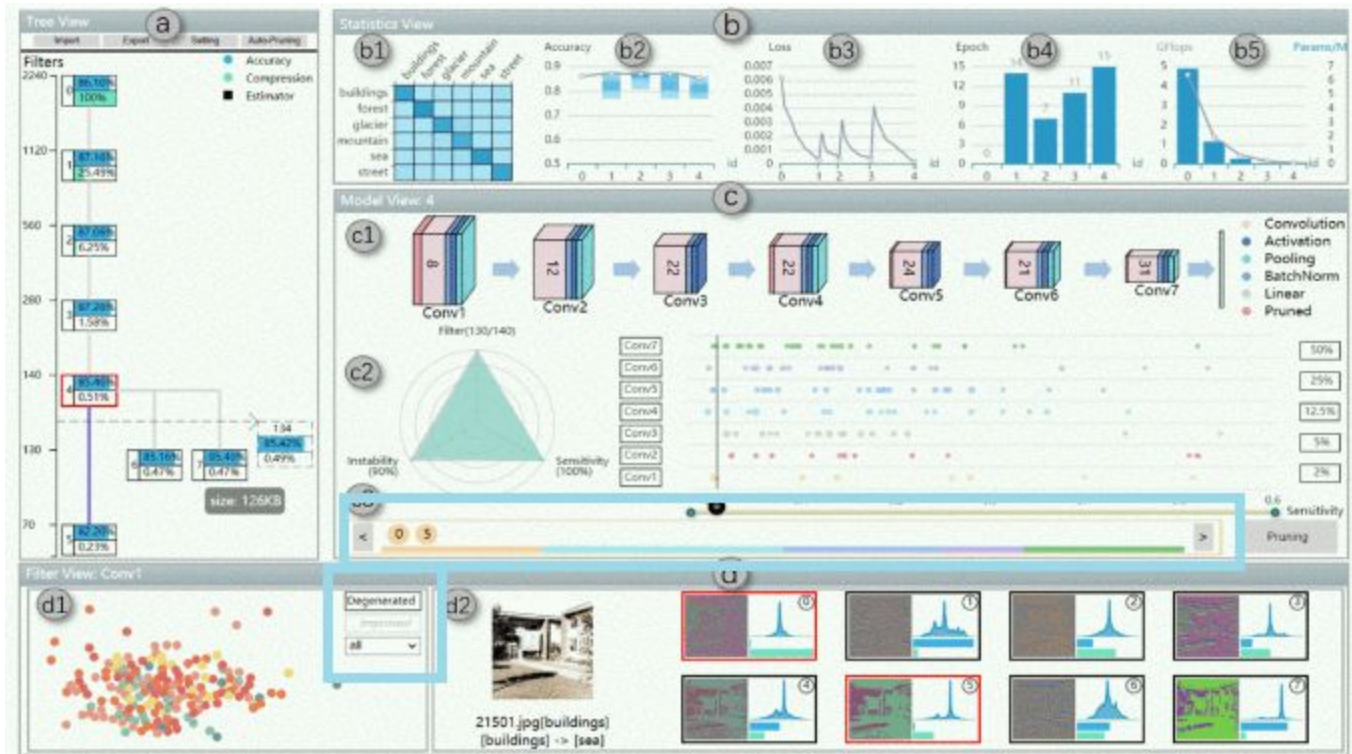


Fig. 3(f) CNNPruner system interface [51] where the user can drag in the bubble plot, can click some nodes of the tree, the cells of the matrix, a layer for convolutional layers or some points in the scatter plot

G. Li et al. Cnnpruner: Pruning convolutional neural networks with visual analytics.

<https://doi.org/10.1109/TVCG.2020.3030461>







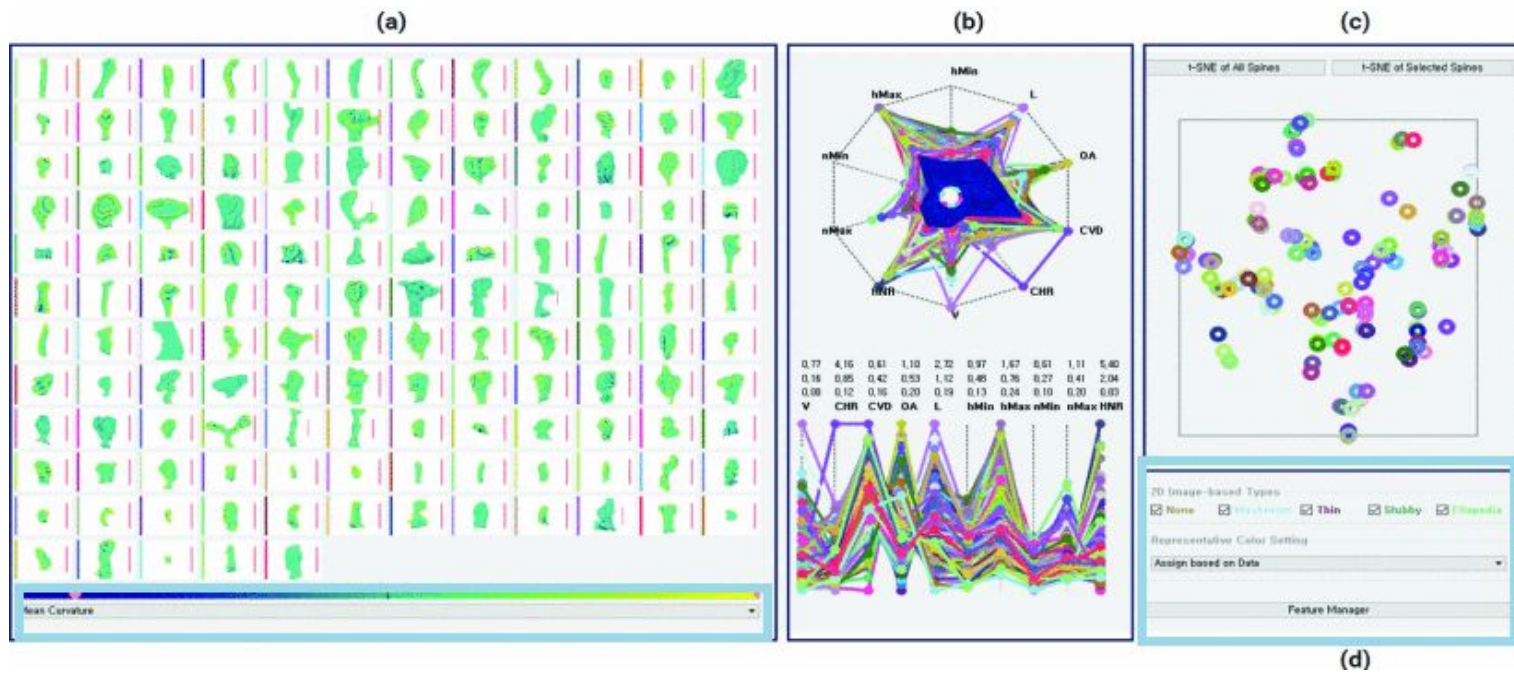


Fig. 4(b) System interface proposed by Choi et al. [64] where the user can click the color bar, a line in the plots, a spine in the grid, can brush more spines on the each axis of plots, furthermore he can select a specific region containing certain spines by dragging the mouse(sect. c) and can rotate the spine by dragging the mouse left(sect. a)

J. Choi et al. Interactive dendritic spine analysis based on 3d morphological features.

<https://doi.org/10.1109/VISUAL.2019.8933795>



Fig. 4(c) System interface proposed by Guo et al. [67] where the filters are shown in section (b) and (d)

S. Guo et al. Interpretable anomaly detection in event sequences via sequence matching and visual comparison.

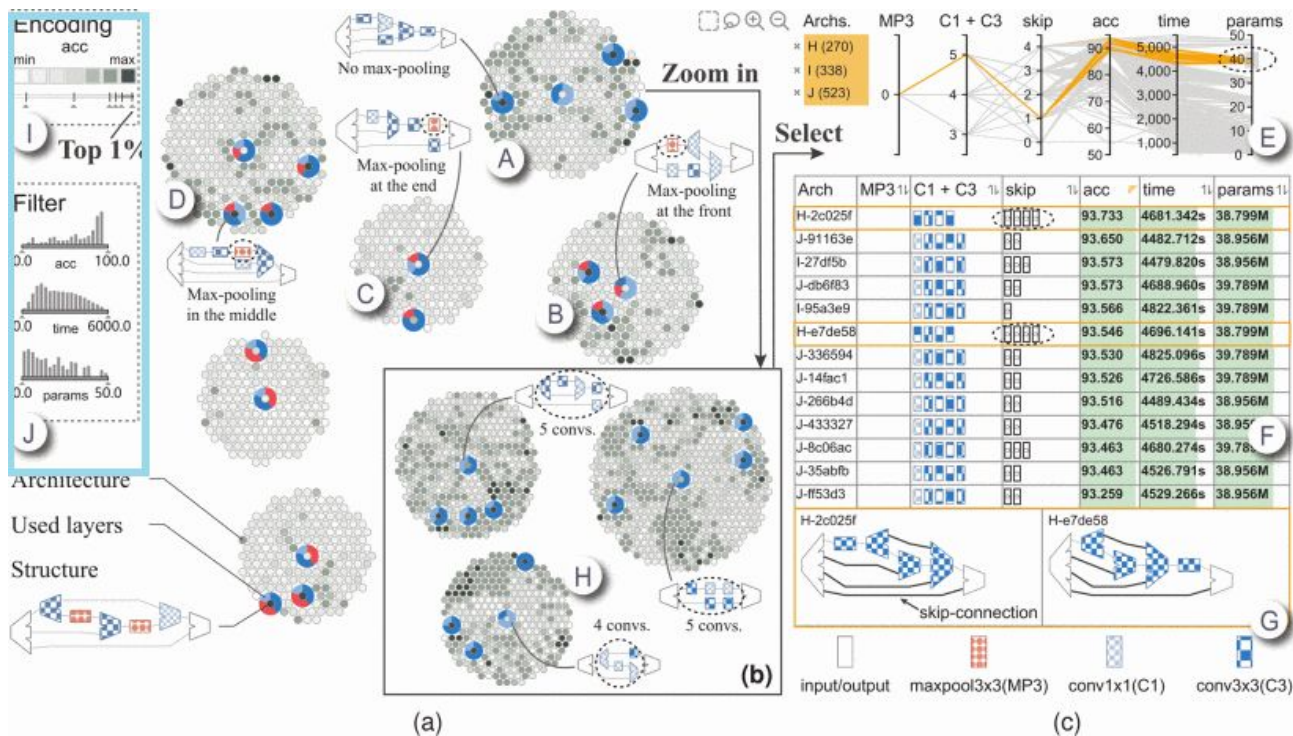
<https://doi.org/10.1109/TVCG.2021.3093585>



Fig. 4(d) System interface proposed by Chen et al. [73] shows in section C, Event Filter, a filter of complex type

Chen et al. Sequence synopsis: Optimize visual summary of temporal event data.

<https://doi.org/10.1109/TVCG.2017.2745083>



J. Yuan et al. Visual analysis of neural architecture spaces for summarizing design principles.

<https://doi.org/10.1109/TVCG.2022.3209404>



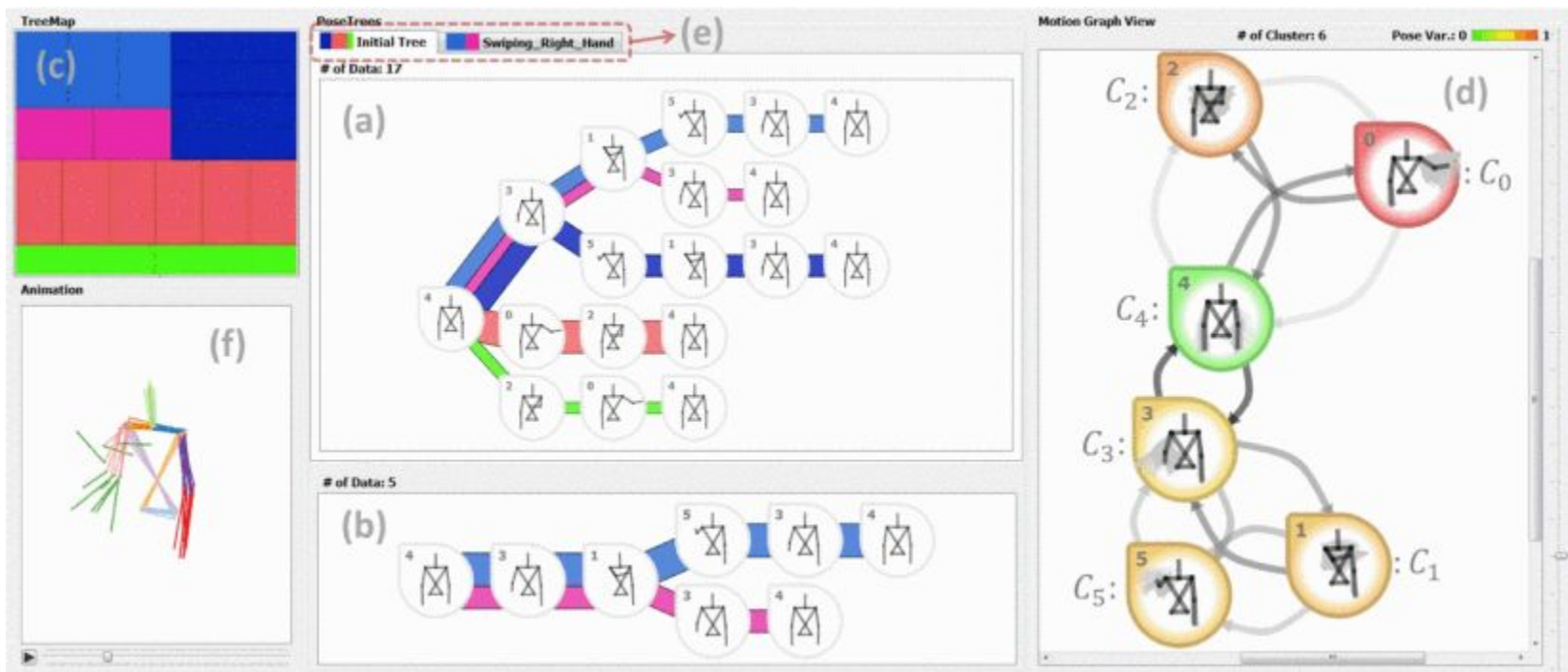


Fig. 4(f) Motionflow system interface [75] where it can be seen that the interface is free of filters

S. Jang et al. Motionflow: Visual abstraction and aggregation of sequential patterns in human motion tracking data.

<https://doi.org/10.1109/TVCG.2015.2468292>



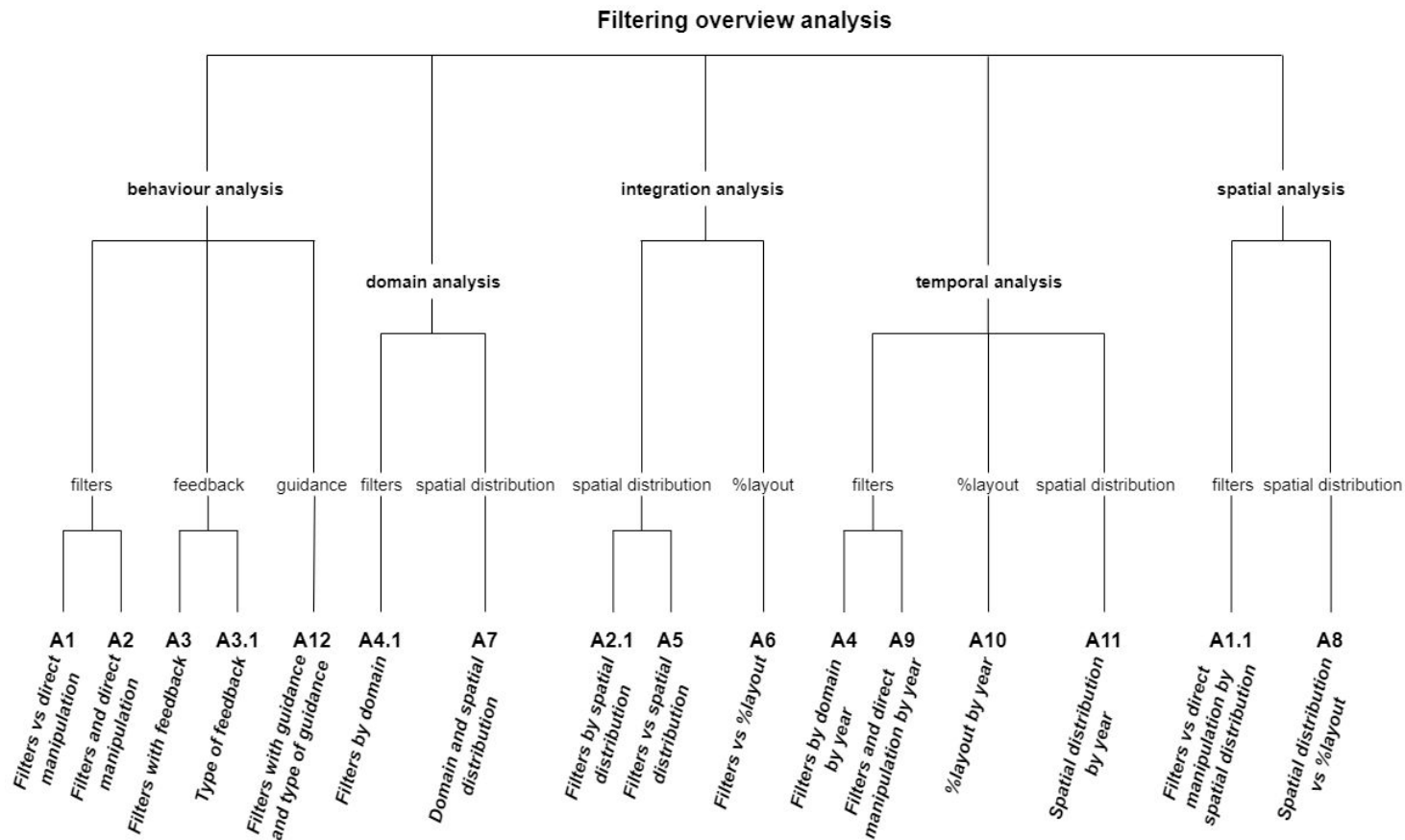
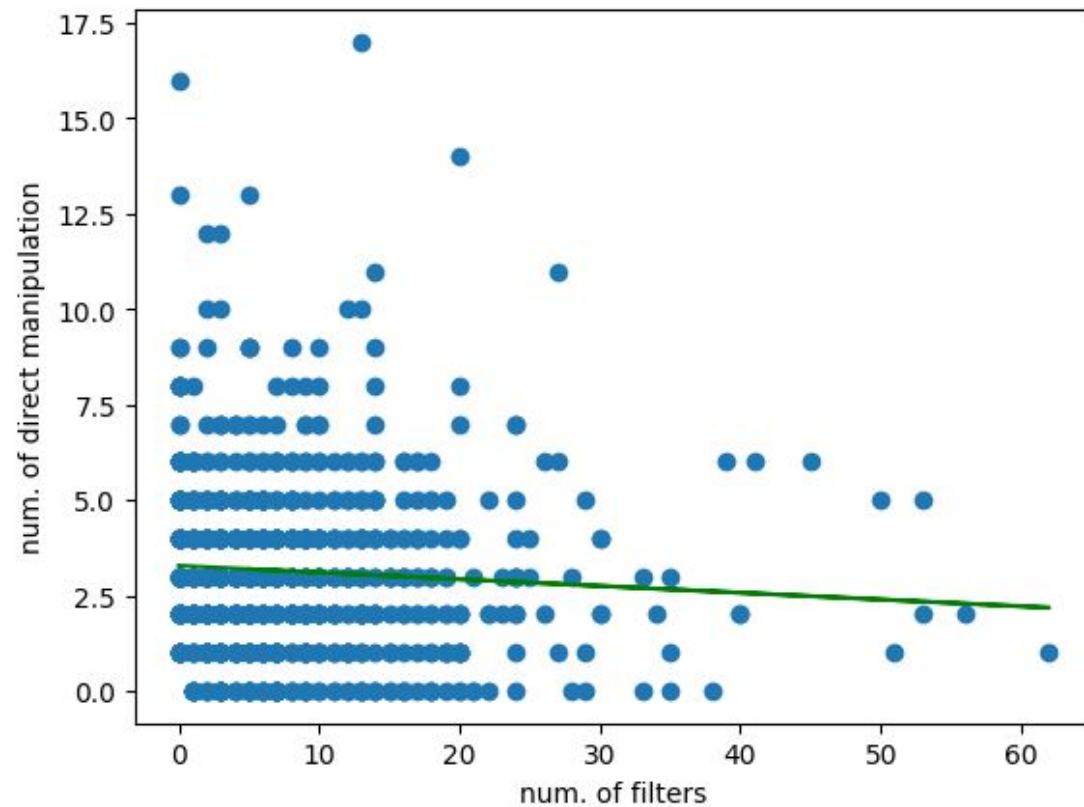


Fig. 5 Overview of the analyzes designed



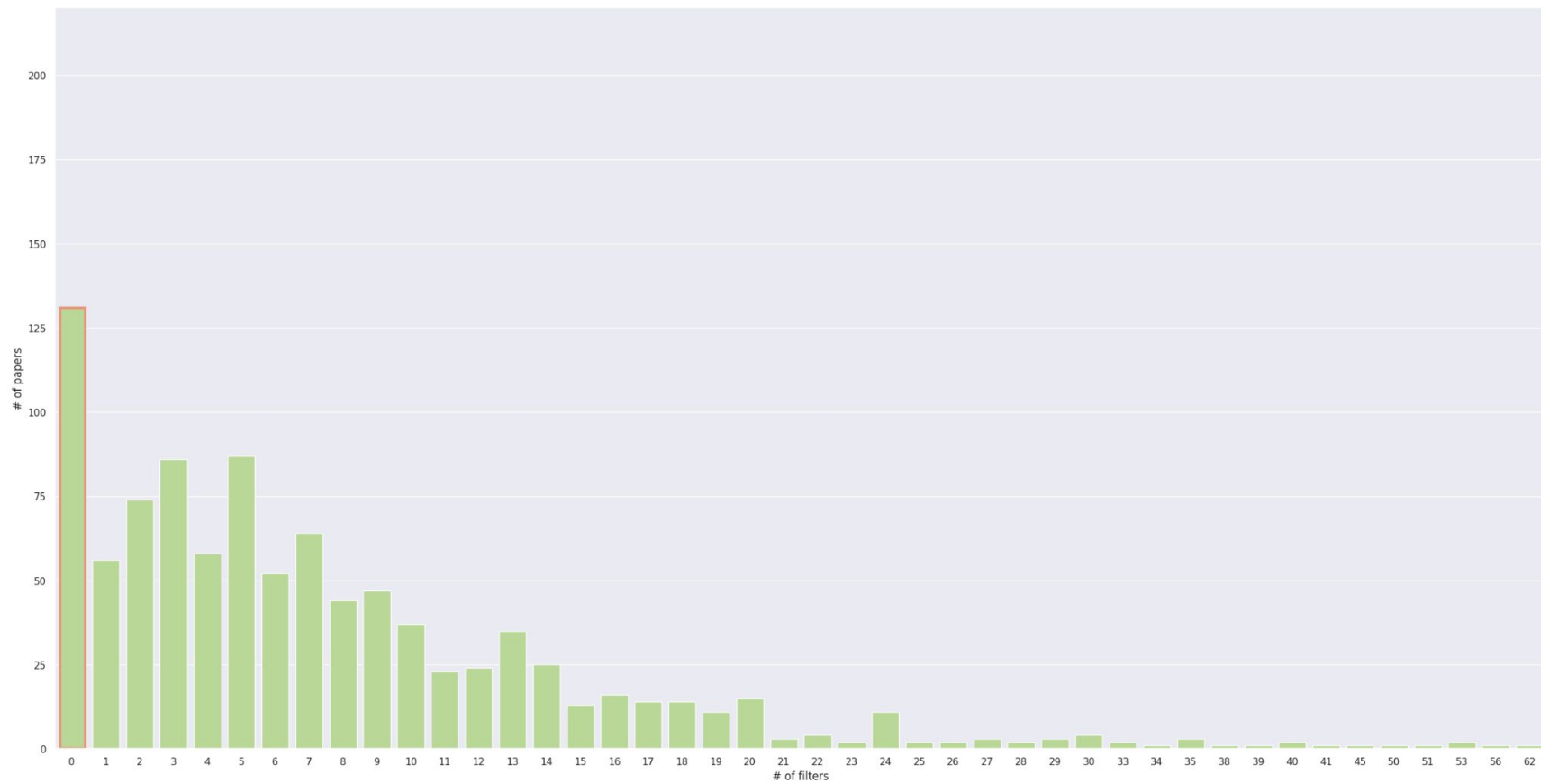


Fig. 6b papers for each number of filters

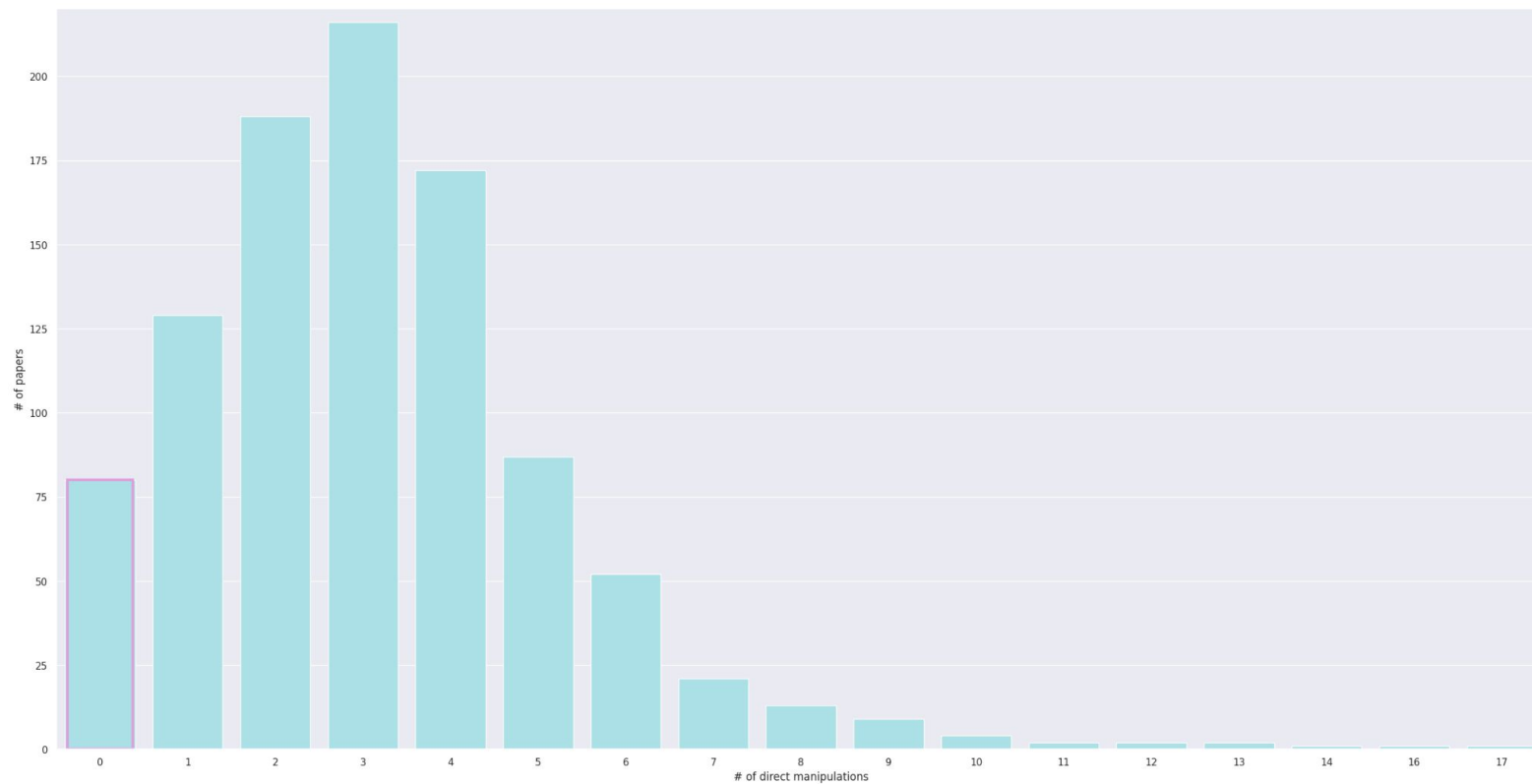


Fig. 6c papers for each number of direct manipulations

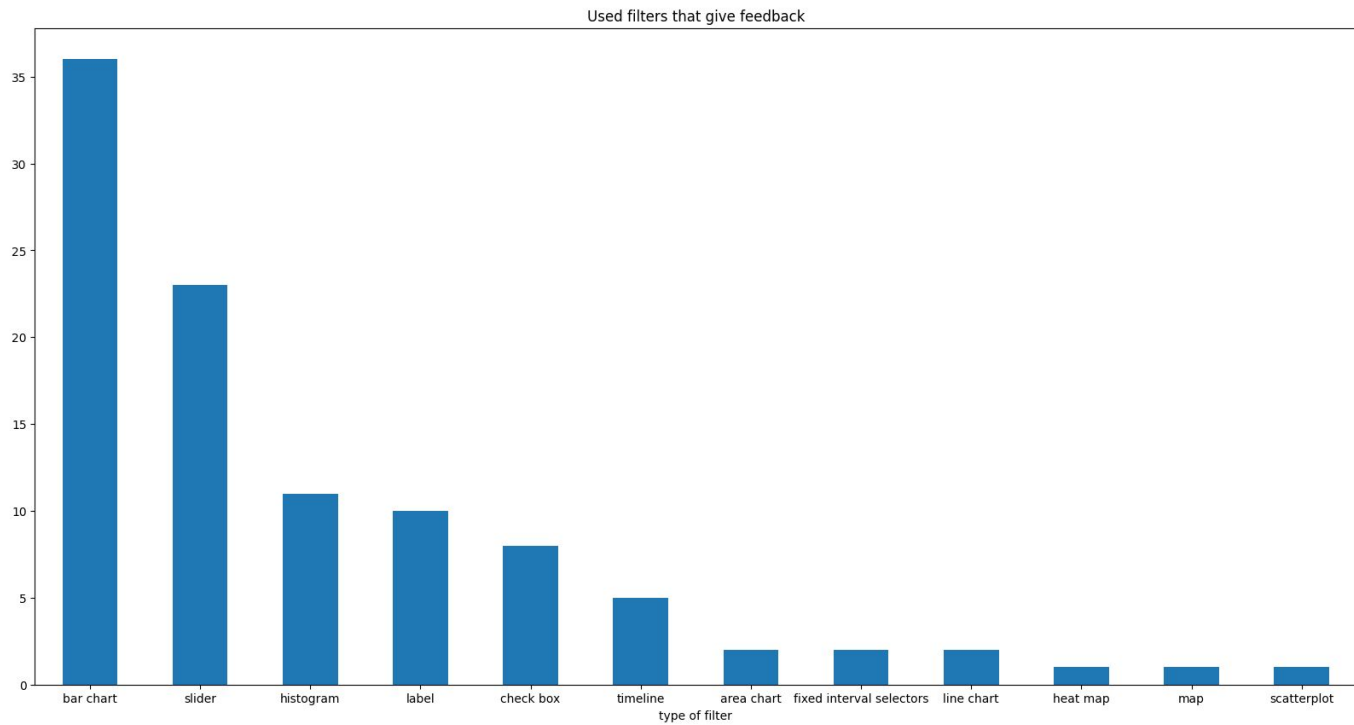


Fig. 6d Types of filters with feedback used



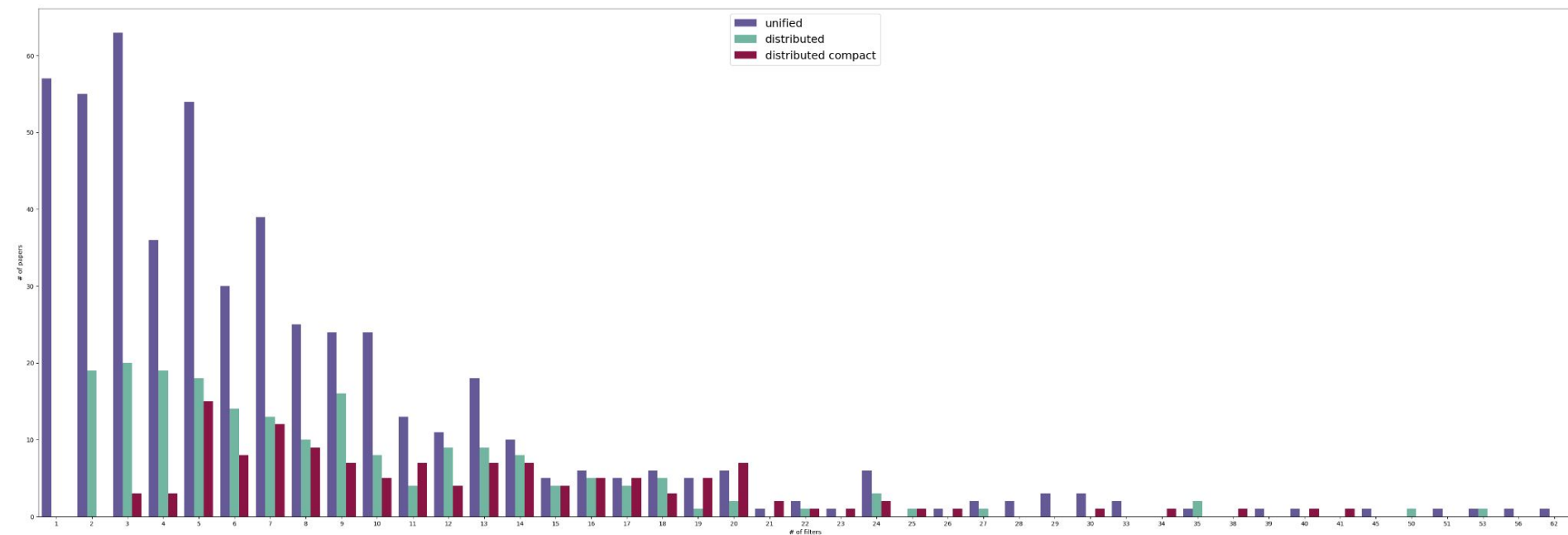


Fig. 7 Distribution of filters divided by spatial distribution

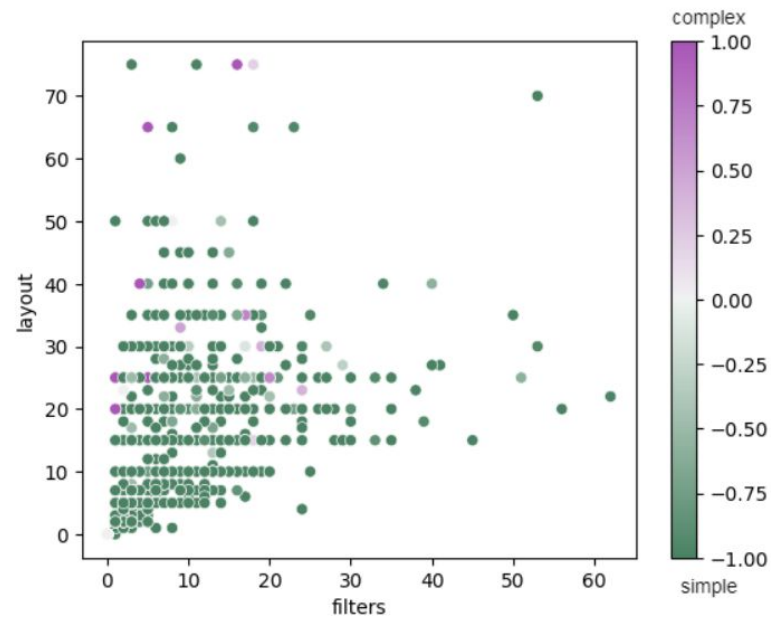
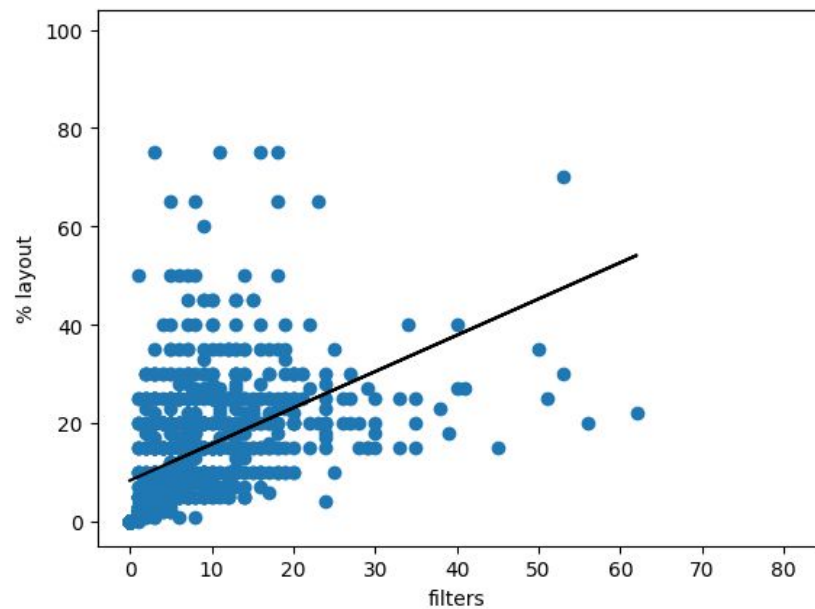


Fig. 8(a) Relationship between filters and occupied space, (b) breakdown by degree of direct manipulation.

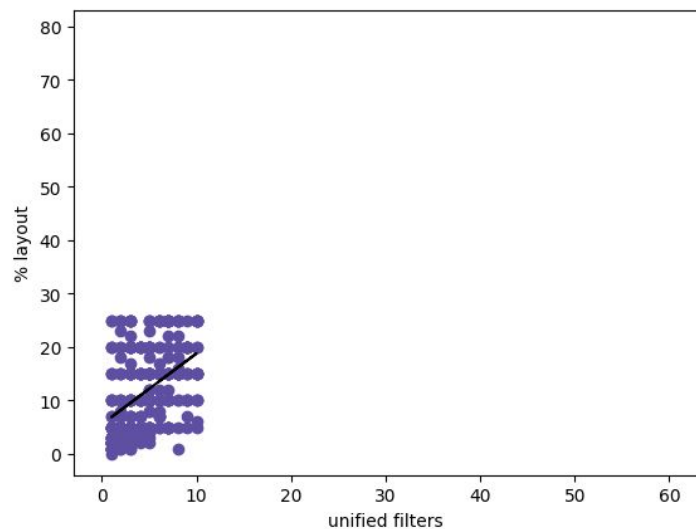
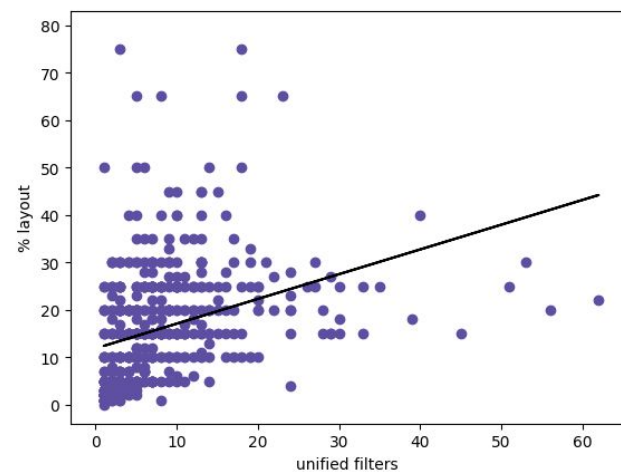
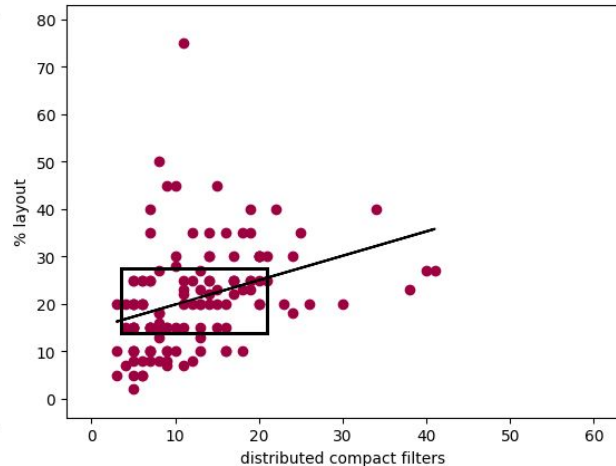
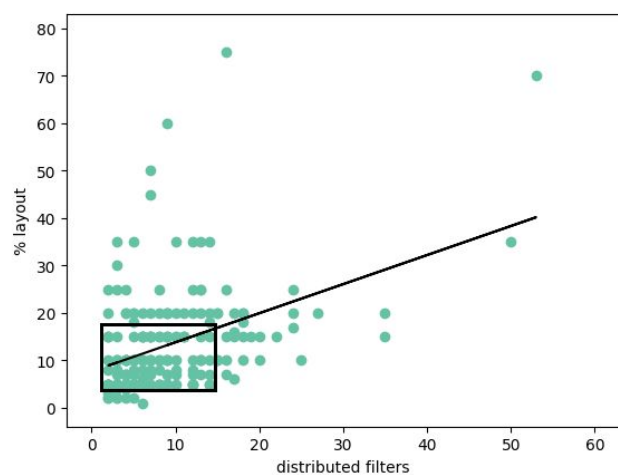


Fig. 9 Relationship between occupied space (%) and: (a) distributed type of filters, (b) distributed compact type of filters and (c) unified type of filters, (d) centered unified filters

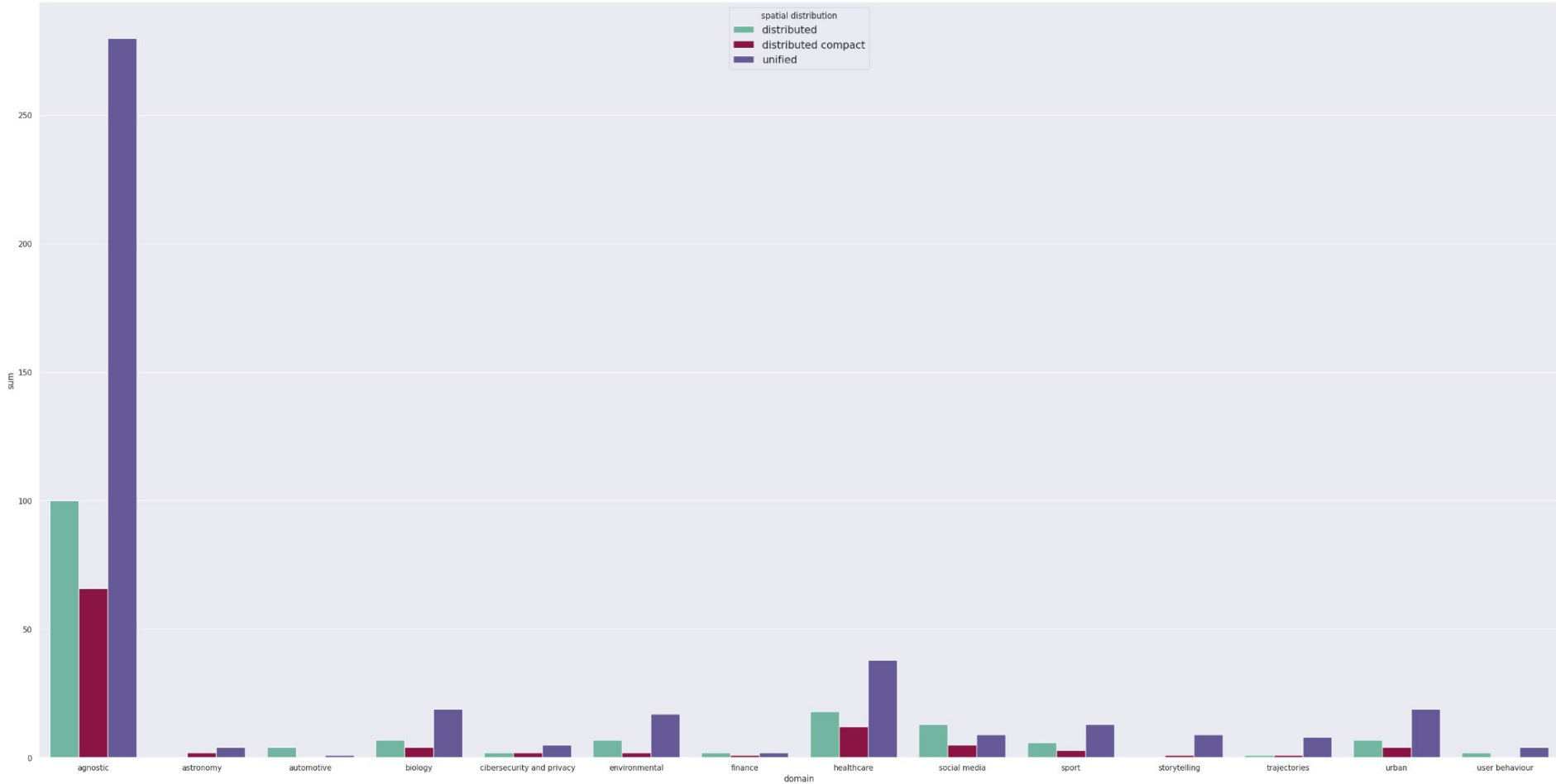


Fig. 10 Spatial distribution of filters (a) for each application domain

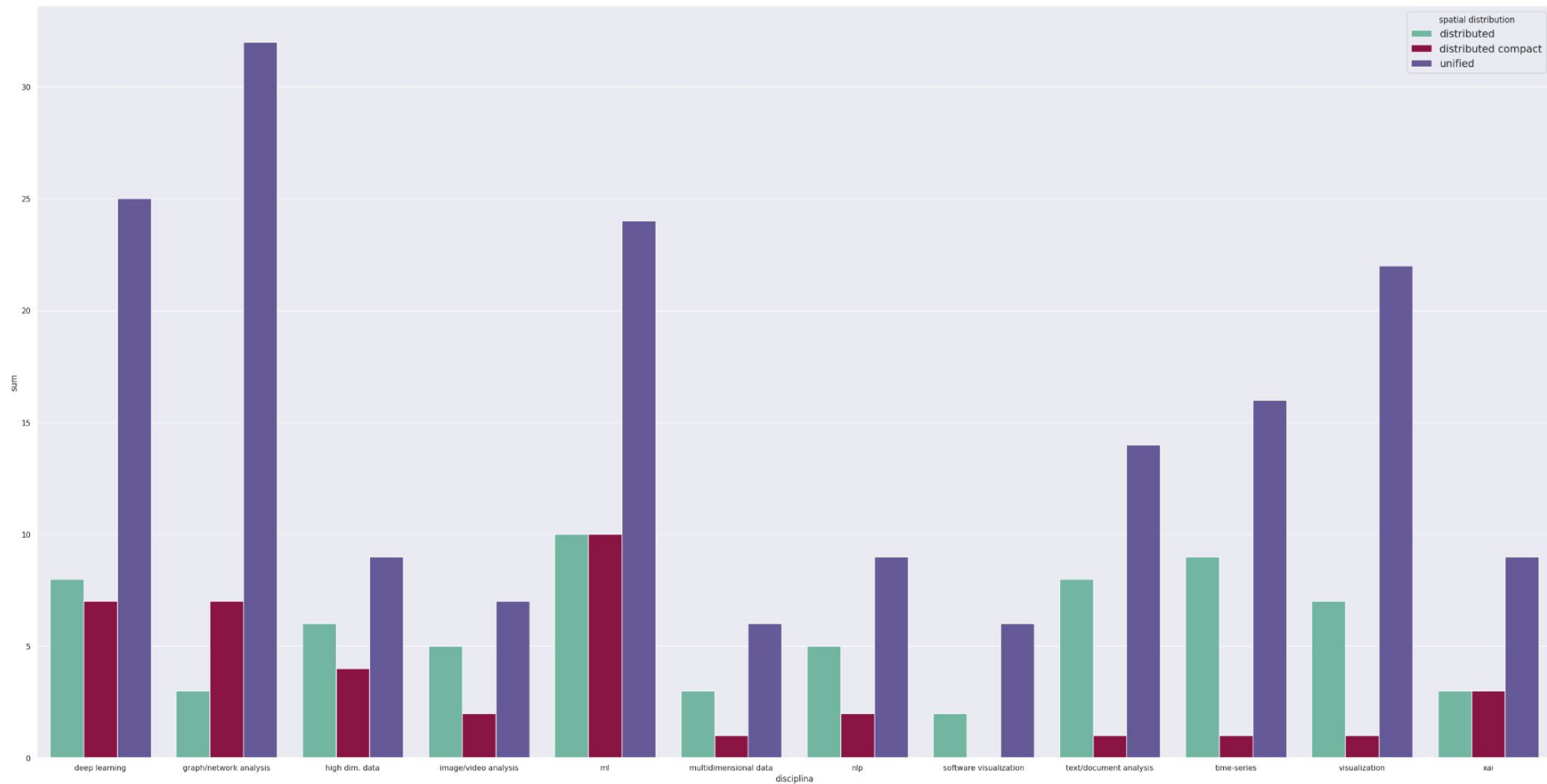


Fig. 10 Spatial distribution of filters (b) for each disciplines



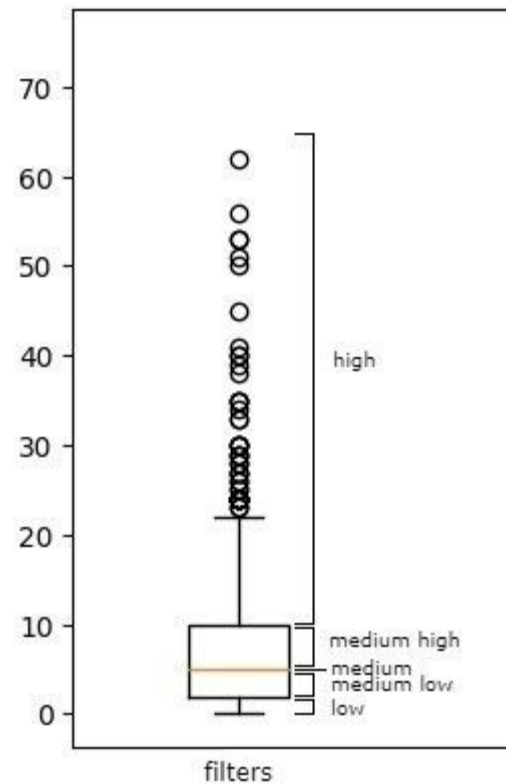
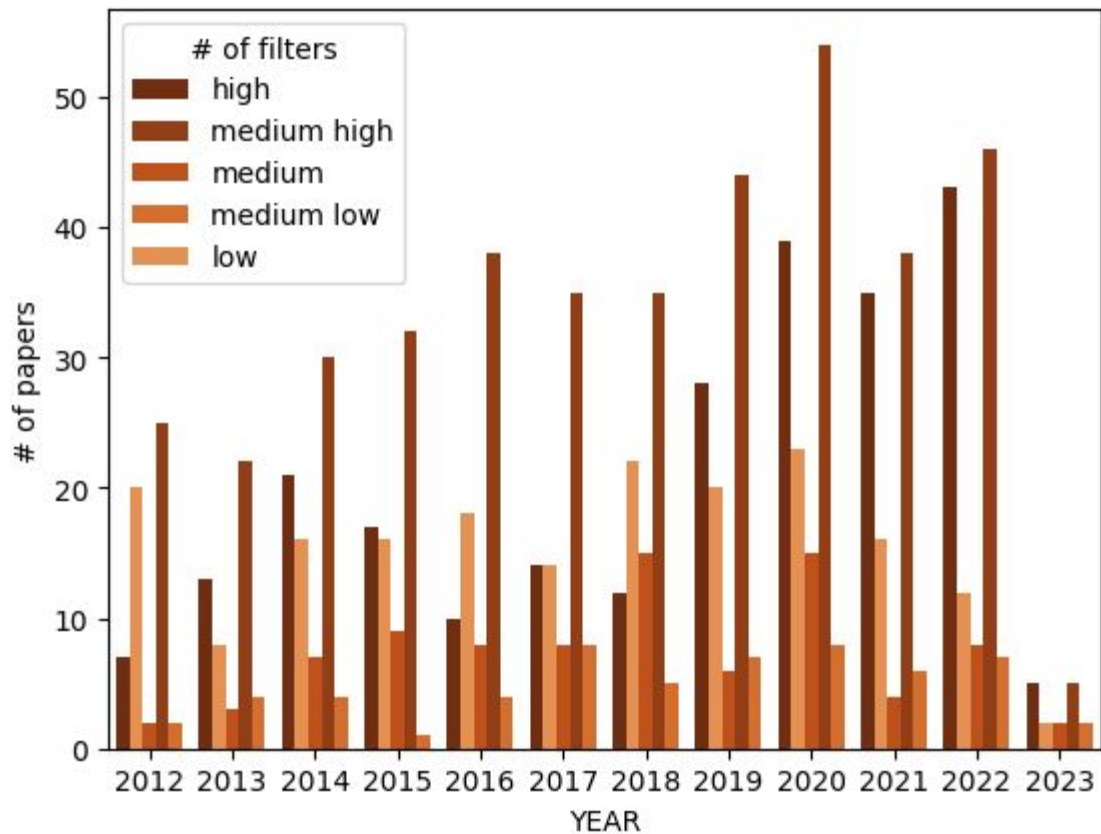


Fig. 11 (a) Bar chart showing the temporal trend of filters(2023 is still in progress so its data is partial), (b) boxplots showing how the five intervals were defined

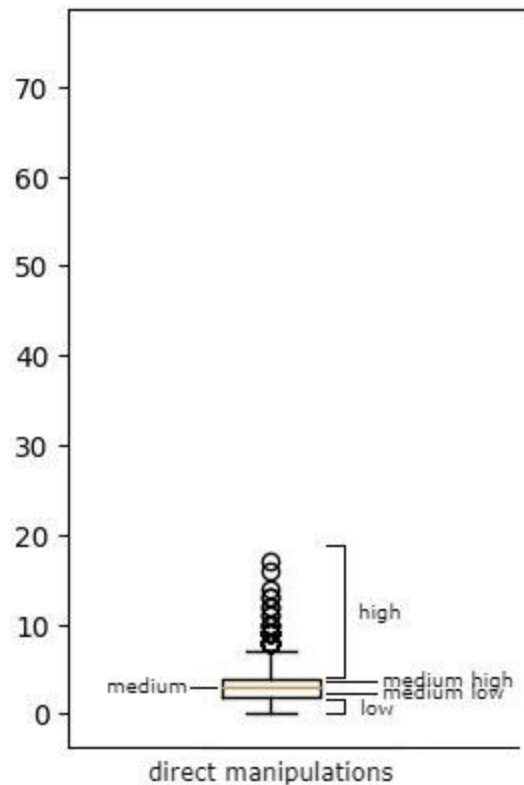
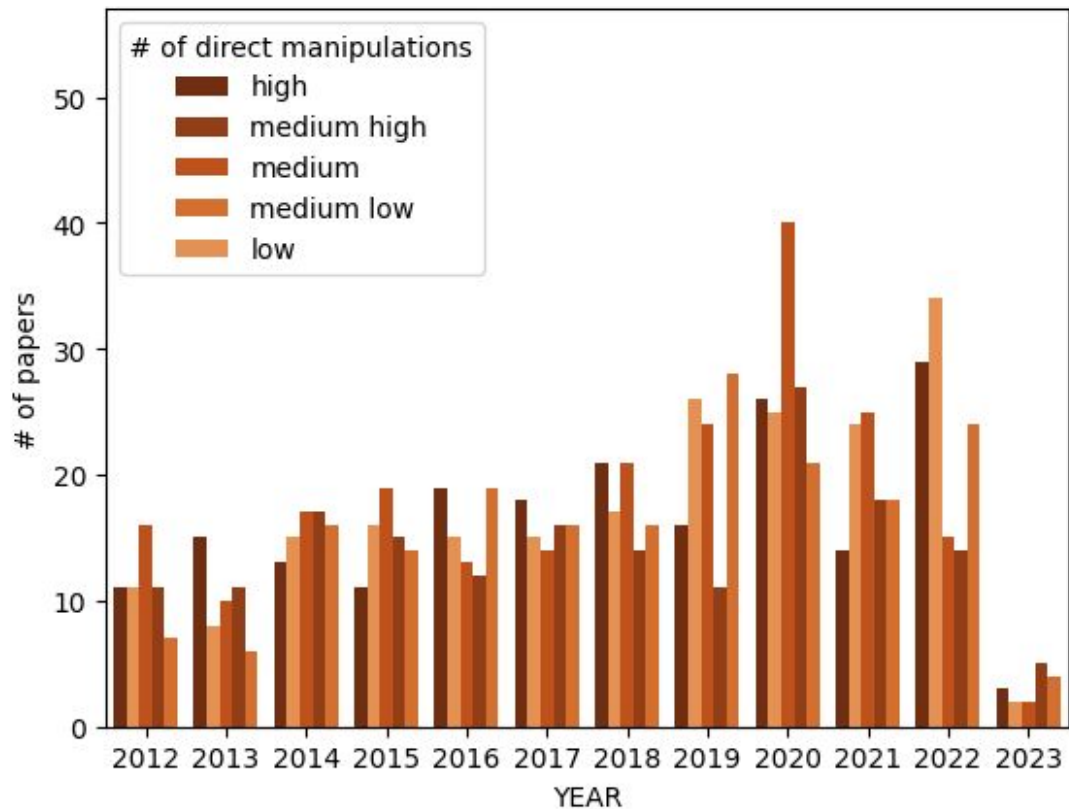


Fig. 11 (c) bar chart showing the temporal trend of direct manipulations (2023 is still in progress so its data is partial), (d) boxplots showing how the five intervals were defined

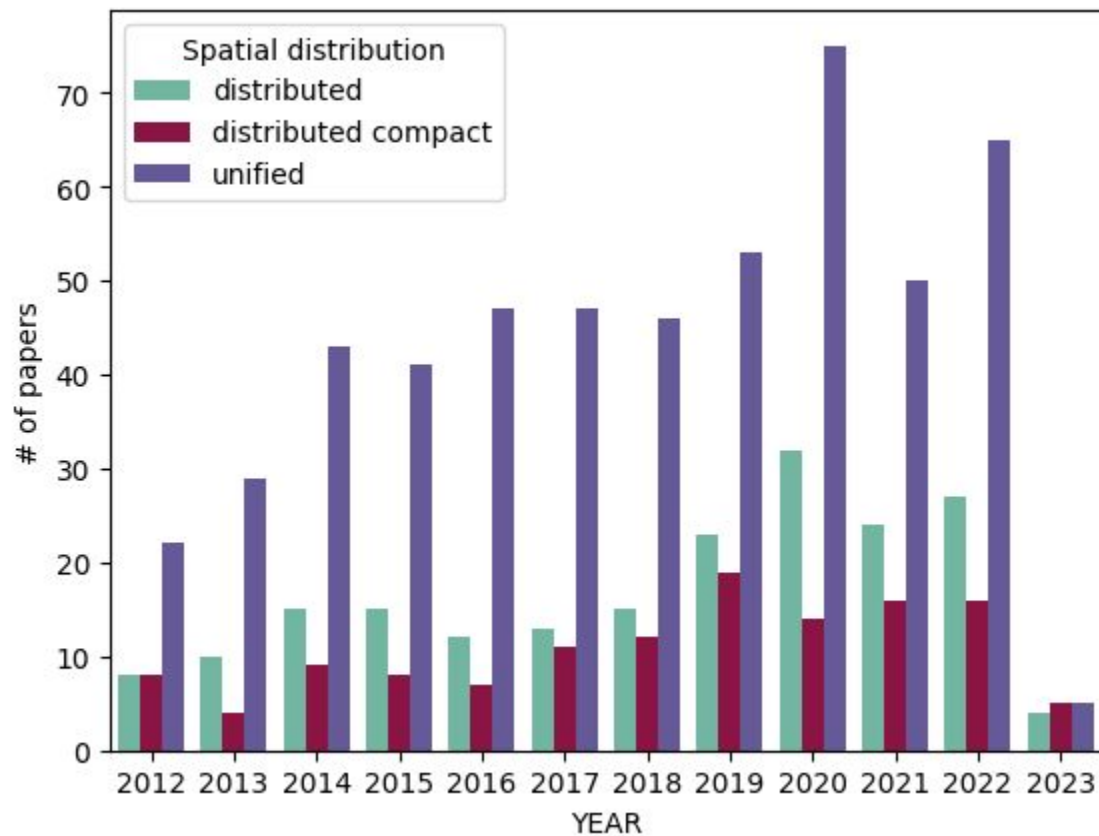


Fig. 12 (a) Temporal distribution of spatial distribution of the filters within the systems

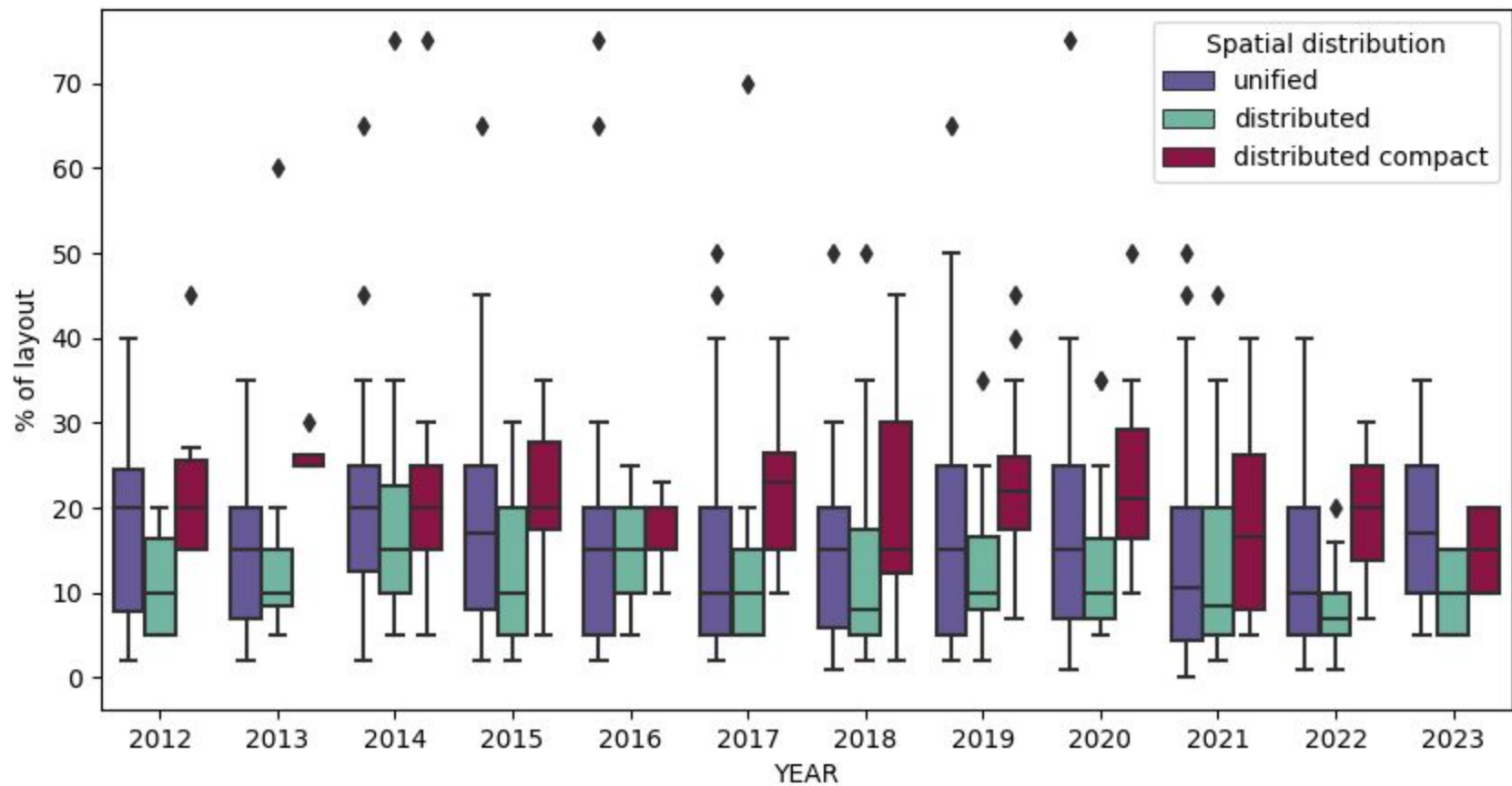


Fig. 12(b) temporal trend of the percentage of layout occupied for each spatial distribution

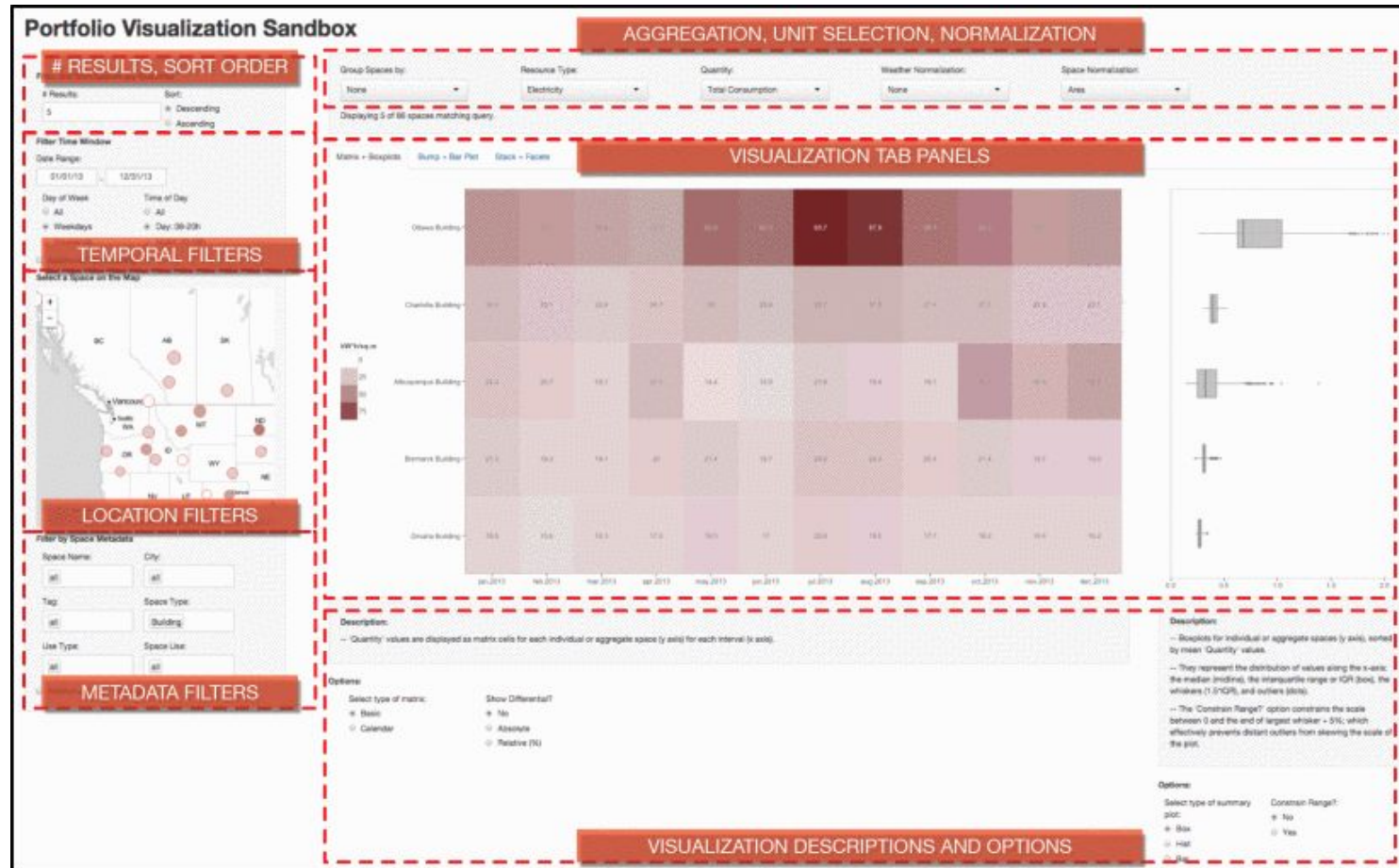


Fig. 13(a) Interface implemented by Brehmer et al. [86], section "LOCATION FILTERS" shows the geomap filter M. Brehmer et al. Matches, mismatches, and methods: Multiple-view workflows for energy portfolio analysis.

<https://doi.org/10.1109/TVCG.2015.2466971>



Fig. 13 (b) DECE system interface [57]: it can be seen that the table occupies most of the visualization so it is not possible to consider it as a filter

F. Cheng et al. Dece: Decision explorer with counterfactual explanations for machine learning models.

<https://doi.org/10.1109/TVCG.2020.3030342>



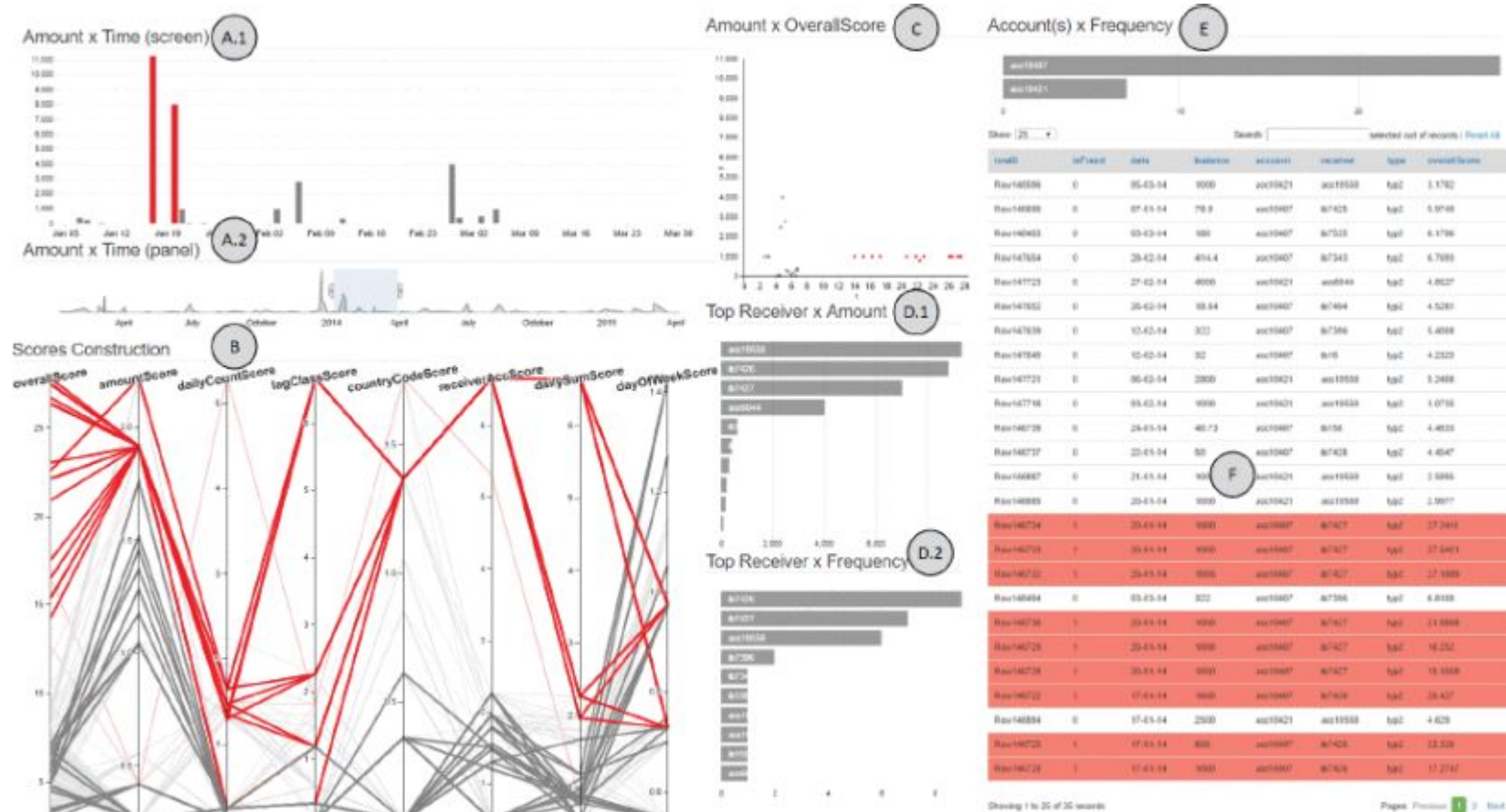


Fig. 14 (a) Eva system interface [95]: section A.2 shows the line-chart which is categorized as a visualization R. A. Leite et al. Eva: Visual analytics to identify fraudulent events.

<https://doi.org/10.1109/TVCG.2017.2744758>



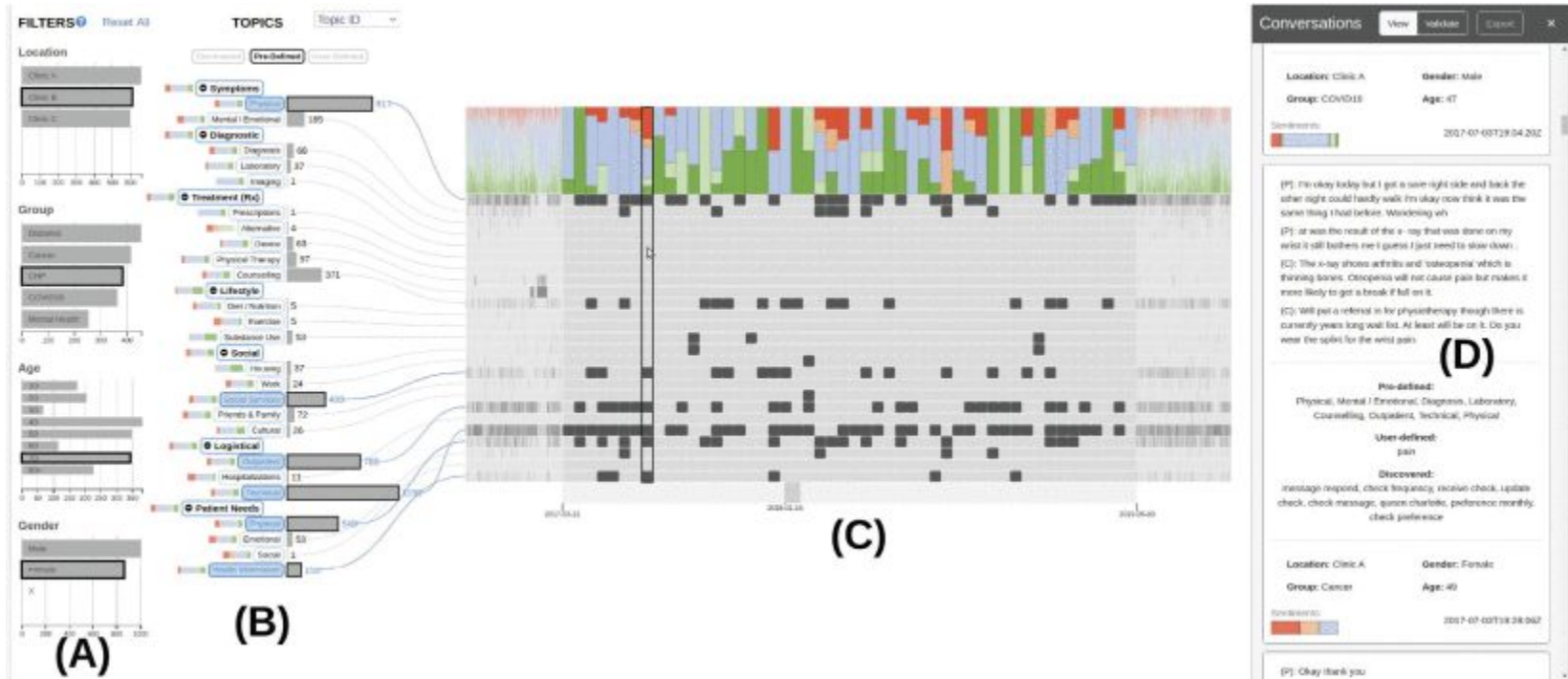


Fig. 14 (b) System interface implemented by Li et al. [96]: section A and B show the implemented cross-filters

R. Li et al. Conviscope: Visual analytics for exploring patient conversations

<https://doi.org/10.1109/VIS49827.2021.9623269>